

Supporting Information

Chiral metal nanoparticles encapsulated by chiral phosphine cavitand with tetrakis-BINAP moiety: their remarkable stability toward ligand exchange and thermal racemization

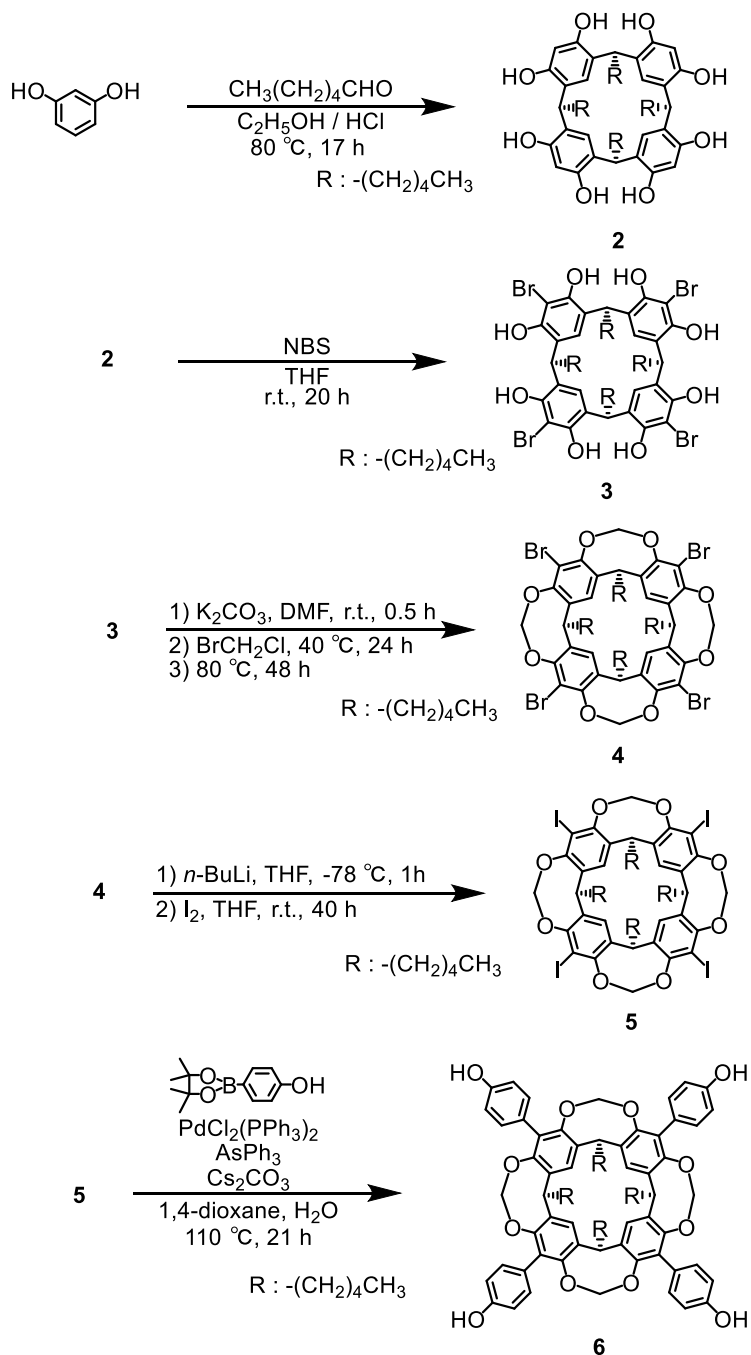
Ryo Nishimura, Ryo Yasutake, Shota Yamada, Koji Sawai, Kazuki Noura,
Tsukasa Nakahodo and Hisashi Fujihara*

*Department of Applied Chemistry, Kinki University, Kowakae,
Higashi-Osaka 577-8502, Japan*

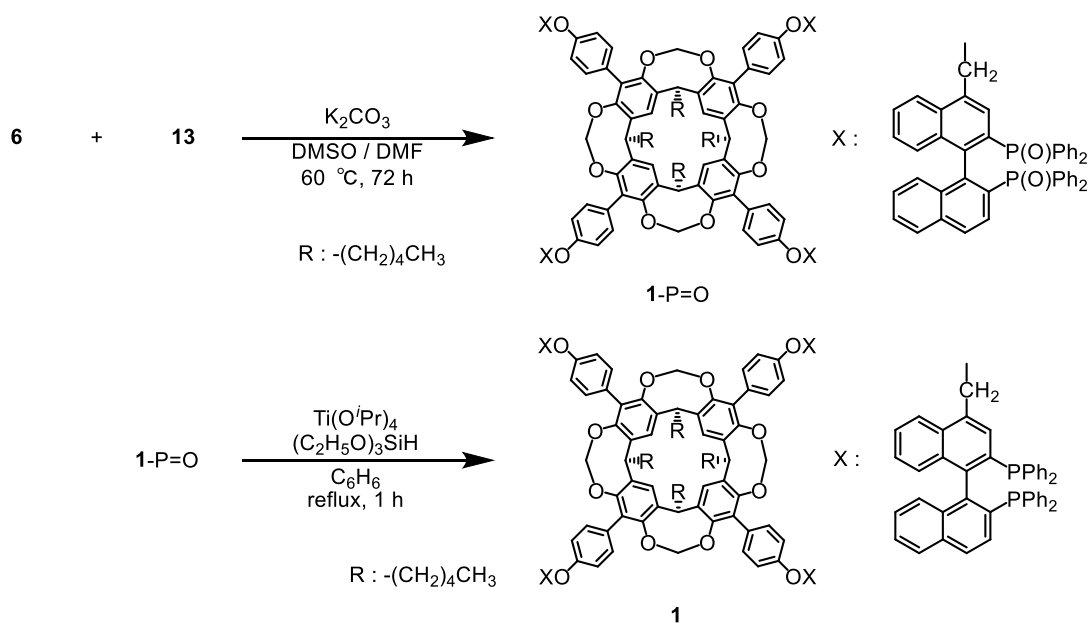
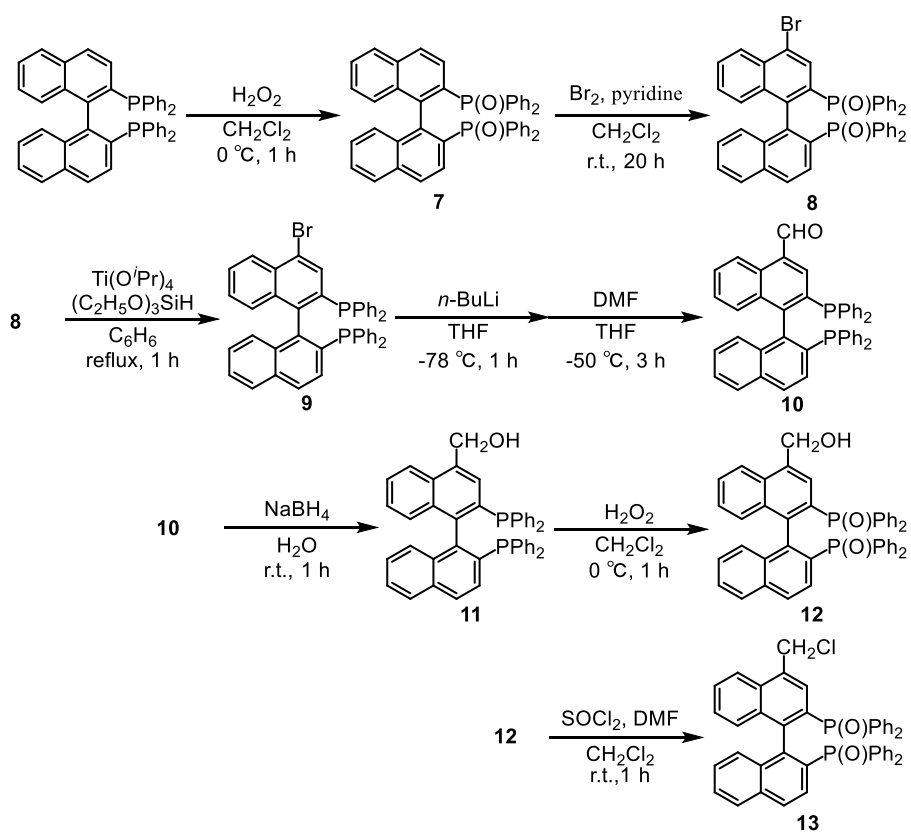
- 1) Synthesis of **1** and **1-P=O**.
- 2) Synthesis of metal nanoparticles (NPs).
- 3) Figures S1-S10.

(1) Synthesis of **1** and **1-P=O**.

Phosphine **1** and the corresponding phosphine-oxide **1-P=O** were synthesized according to Schemes S1 and S2.



Scheme S1



Scheme S2

6: FT-IR (cm^{-1} , KBr) 3448 (O-H); $^1\text{H-NMR}$ (400 MHz, DMSO-d_6) δ 0.90 (t, 12H, $-\text{CH}_3$), 1.29-1.45 (m, 24H, $-(\text{CH}_2)_3-\text{CH}_3$), 2.45 (m, 8H, $-\text{CH}_2-(\text{CH}_2)_3-\text{CH}_3$), 4.24 (d, 4H, $-\text{OCH}_2\text{O}-$), 4.66 (t, 4H, $-\text{CH}-$), 5.17 (d, 4H, $-\text{OCH}_2\text{O}-$), 6.68 (d, 8H, Ar-H), 6.84 (d, 8H, Ar-H), 7.70 (s, 4H, Ar-H); $^{13}\text{C-NMR}$ (100 MHz, DMSO-d_6) δ 14.0 ($-(\text{CH}_2)_4-\text{CH}_3$), 22.3, 27.4, 29.6, 31.5 ($-(\text{CH}_2)_4-\text{CH}_3$), 37.2 ($-\text{CH}-$), 99.7 ($-\text{OCH}_2\text{O}-$), 114.6, 120.9, 123.6, 129.0, 131.1, 138.0, 152.0, 156.2 (Ar); MS (FAB) m/z 1186 (MH^+).

13: FT-IR (cm^{-1} , KBr) 1437 (P-Ph), 1199 (P=O); $^1\text{H-NMR}$ (400 MHz, CDCl_3) δ 4.82, (d, 1H, $-\text{CH}_2\text{-Cl}$), 5.19 (d, 1H, $-\text{CH}_2\text{-Cl}$), 6.79-6.87 (m, 4H, Ar-H), 7.22-7.48 (m, 20H, Ar-H), 7.65-7.72 (m, 4H, Ar-H), 7.79-7.86 (m, 2H, Ar-H), 8.11 (d, 1H, Ar-H); $^{13}\text{C-NMR}$ (100 MHz, CDCl_3) δ 44.7 (CH_2Cl), 123.4, 125.9, 127.1, 127.2, 127.4, 127.5, 127.7, 127.8, 127.9, 128.0, 128.1, 128.2, 129.5, 129.7, 130.9, 131.0, 131.2, 131.3, 131.8, 131.9, 132.0, 132.4, 132.5, 133.8, 134.0, 134.7, 134.9 (Ar); MS (FAB) m/z 703 (M^+).

1-P=O: FT-IR (cm^{-1} , KBr) 1437 (P-Ph), 1207 (P=O); $^1\text{H-NMR}$ (400 MHz, CDCl_3) δ 0.97 (t, 12H, $-\text{CH}_3$), 1.42-1.49 (m, 24H, $-(\text{CH}_2)_3-\text{CH}_3$), 2.37 (m, 8H, $-\text{CH}_2-(\text{CH}_2)_3-\text{CH}_3$), 4.33 (d, 4H, $-\text{OCH}_2\text{O}-$), 4.90 (t, 4H, $-\text{CH}-(\text{CH}_2)_4-$), 5.21 (d, 4H, $-\text{CH}_2\text{O}-$), 5.37 (d, 4H, $-\text{OCH}_2\text{O}-$), 5.55 (d, 4H, $-\text{CH}_2\text{O}-$), 6.75-7.99 (m, Ar-H); $^{13}\text{C-NMR}$ (100 MHz, CDCl_3) δ 14.2 ($-\text{CH}_3$), 22.7, 27.7, 30.5, 32.1, 37.2, 68.8 ($-\text{CH}_2-$), 100.7 ($-\text{OCH}_2\text{O}-$), 114.2, 119.6, 123.6, 125.8, 126.5, 127.2, 127.7, 127.8, 127.9, 128.0, 128.1, 128.2, 128.3, 128.8, 130.0, 130.8, 131.0, 131.2, 131.3, 131.8, 131.9, 132.0, 132.2, 132.3, 132.4, 132.5, 133.1, 133.2, 133.3, 133.5, 133.7, 133.8, 133.9, 134.6, 134.8, 148.9, 152.8, 154.2, 157.8 (Ar); $^{31}\text{P-NMR}$ (202 MHz, CDCl_3) δ 28.6, 29.2 [$^{31}\text{P-NMR}$ of the phosphine-oxide of BINAP (CDCl_3) δ 28.9]; MS (FAB) m/z 3852 (M^+).

1: FT-IR (cm^{-1} , KBr) 1433 (P-Ph); $^1\text{H-NMR}$ (400 MHz, CDCl_3) δ 0.95 (t, 12H, $-\text{CH}_3$), 1.38-1.47 (m, 24H, $-(\text{CH}_2)_3-\text{CH}_3$), 2.35 (m, 8H, $-\text{CH}_2-(\text{CH}_2)_3-\text{CH}_3$), 4.30 (d, 4H, $-\text{OCH}_2\text{O}-$), 4.88 (t, 4H, $-\text{CH}-$), 5.29 (d, 4H, $-\text{CH}_2\text{O}-$), 5.34 (d, 4H, $-\text{OCH}_2\text{O}-$), 5.46 (d, 4H, $-\text{CH}_2\text{O}-$), 6.60-8.09 (m, Ar-H); $^{31}\text{P-NMR}$ (202 MHz, CDCl_3) δ -15.0, -14.9 [$^{31}\text{P-NMR}$ of the phosphine of BINAP (CDCl_3) δ -14.9].

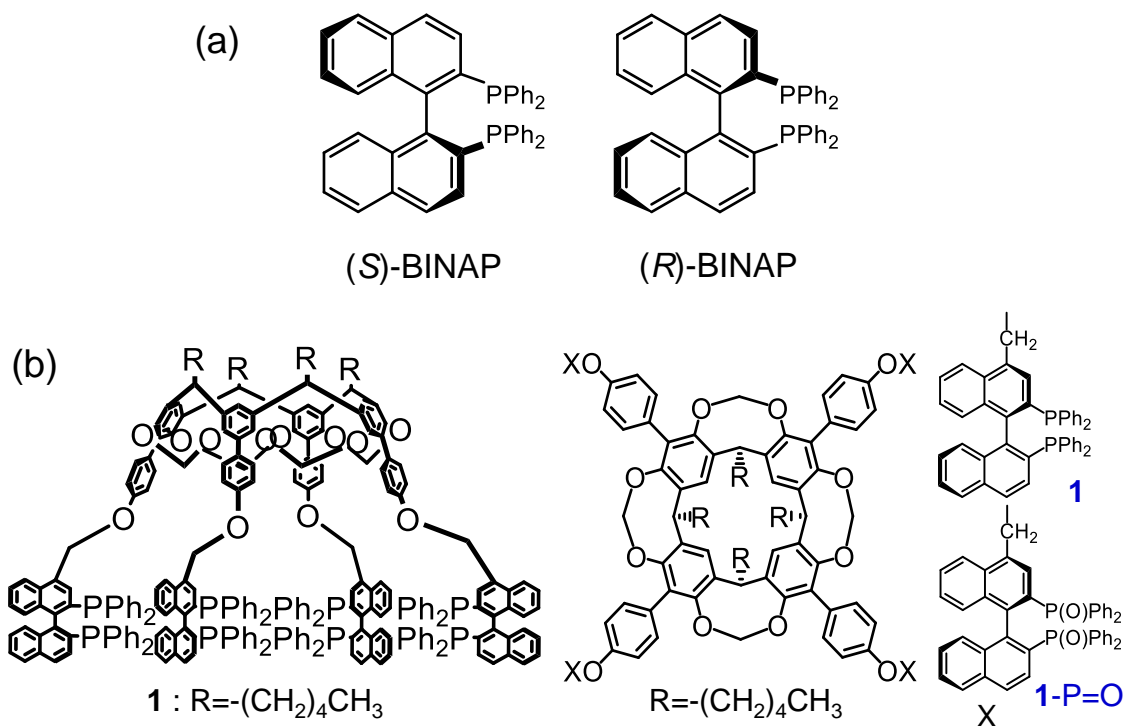


Chart S1. Structures of (R)-BINAP, (S)-BINAP, **1** and 1-P=O.

(2) Synthesis of chiral metal NPs.

The chiral phosphine cavitand **1**-protected gold NPs were prepared as follows. To a vigorously stirred solution of HAuCl₄·4H₂O (16 mg, 0.04 mmol) in 7 mL of deionized water under an argon atmosphere was added the chiral phosphine **1** (120 mg, 0.032 mmol) in 30 mL of THF. A solution of NaBH₄ (16 mg, 0.43 mmol) in 6 mL of deionized water was added at 0 °C, and the resulting mixture was stirred for 1 h at room temperature under an argon atmosphere. After the reaction, the filtrate was evaporated in vacuo to yield the chiral phosphine cavitand **1**-protected gold NPs (**1**-Au NPs). Purification (dichloromethane-*n*-hexane) of the **1**-Au NPs was repeated until no free phosphine remained, as detected by TLC, ¹H and ¹³C NMR spectroscopies. The X-ray photoelectron spectroscopy (XPS) spectrum of the **1**-Au NPs showed the Au 4f binding energies at 84.2 and 87.9 eV, corresponding to the Au⁰ state. There was a feature at

285 eV due to C 1s and 132 eV due to P 2p. The **1**-Au NPs are remarkably stable both in solution, as well as in the solid state. The number of gold atoms and the ligand in the **1**-protected Au NPs is roughly estimated to be ~21 for gold atoms and ~9 for the ligand. A detailed characterization is currently in progress. The other metal (Ru, Rh, Pd, Ag, and Pt) NPs were prepared by similar methods.

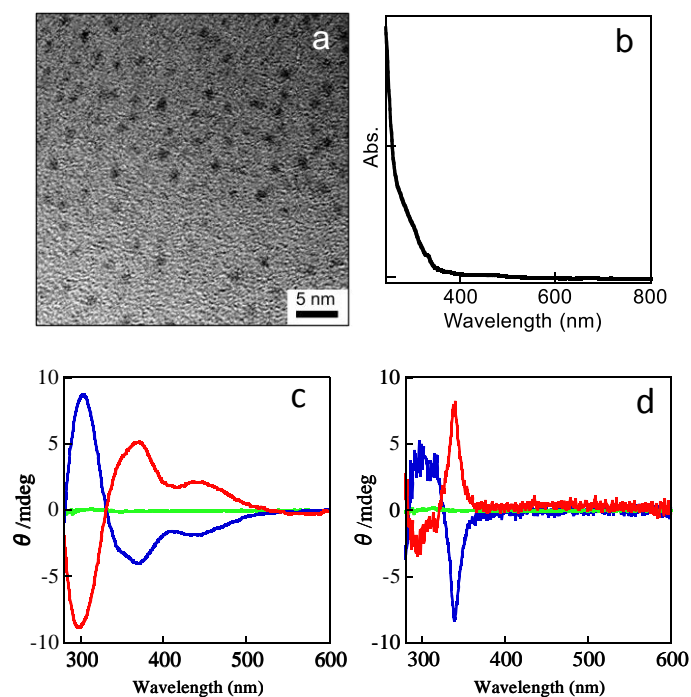


Figure S1. a) TEM image of **1**-Au NPs, b) UV-vis spectrum of **1**-Au NPs in CH_2Cl_2 , c) CD spectrum of **1**-Au NPs in CHCl_3 , and d) CD spectrum of **1** in CHCl_3 .

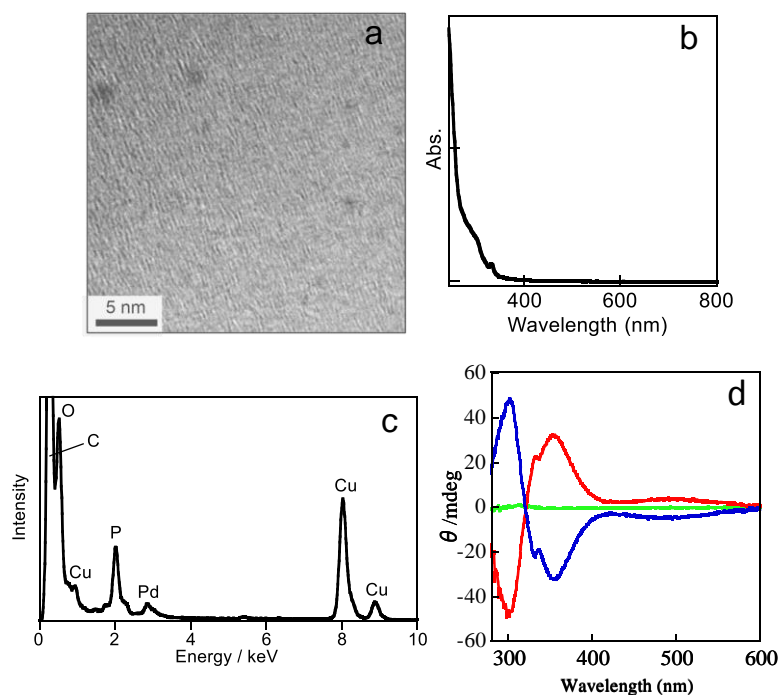


Figure S2. 1-Pd NPs: a) TEM image, b) UV-vis spectrum in CH_2Cl_2 , c) EDX spectrum. Cu peaks are from the supporting copper grid, and d) CD spectra in CHCl_3 .

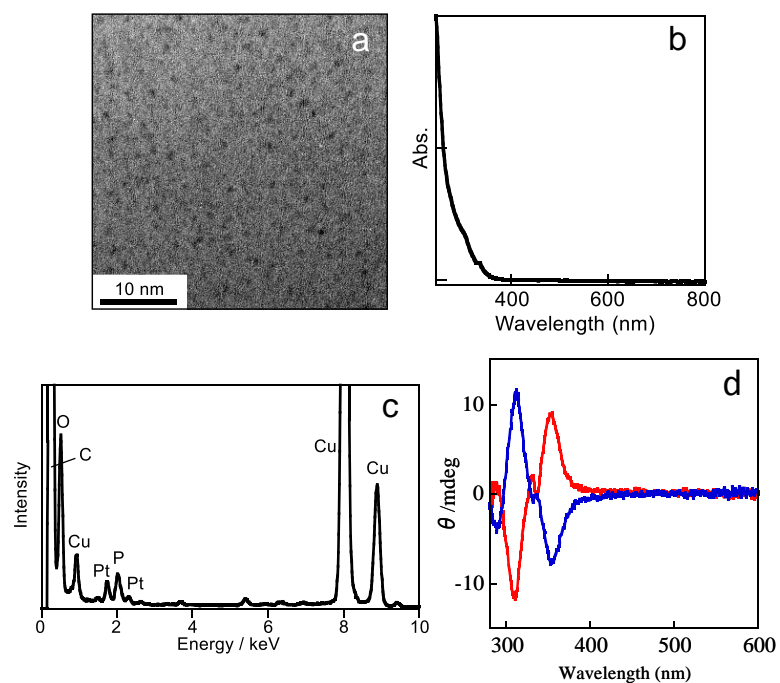


Figure S3. 1-Pt NPs: a) TEM image, b) UV-vis spectrum in CH_2Cl_2 , c) EDX spectrum. Cu peaks are from the supporting copper grid, and d) CD spectra in CHCl_3 .

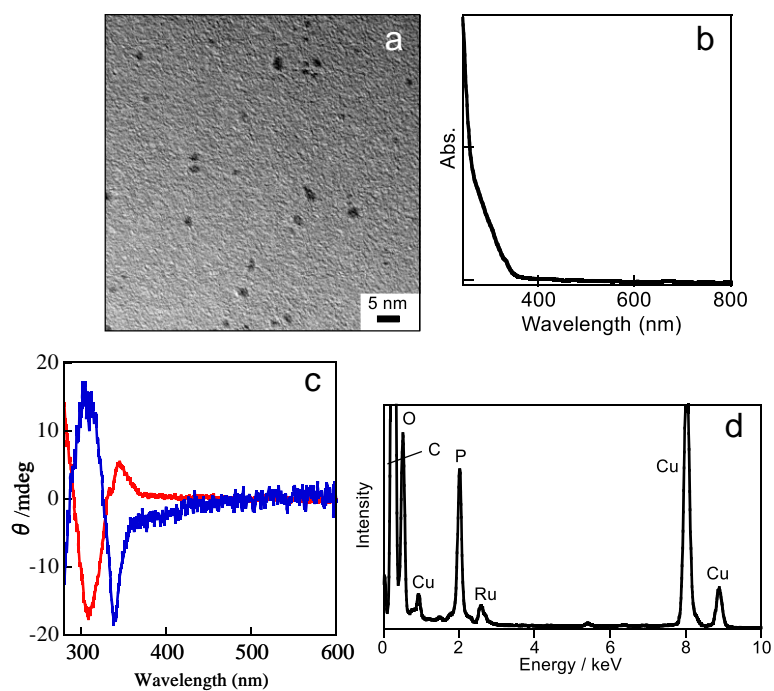


Figure S4. 1-Ru NPs: a) TEM image, b) UV-vis spectrum in CH_2Cl_2 , c) CD spectra in CHCl_3 , and d) EDX spectrum. Cu peaks are from the supporting copper grid.

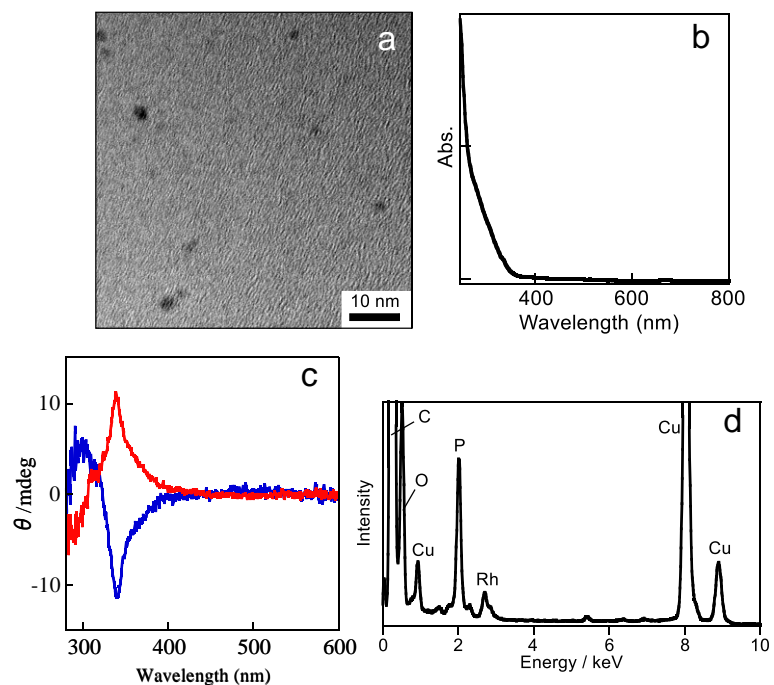


Figure S5. 1-Rh NPs: a) TEM image, b) UV-vis spectrum in CH_2Cl_2 , c) CD spectra in CHCl_3 , and d) EDX spectrum. Cu peaks are from the supporting copper grid.

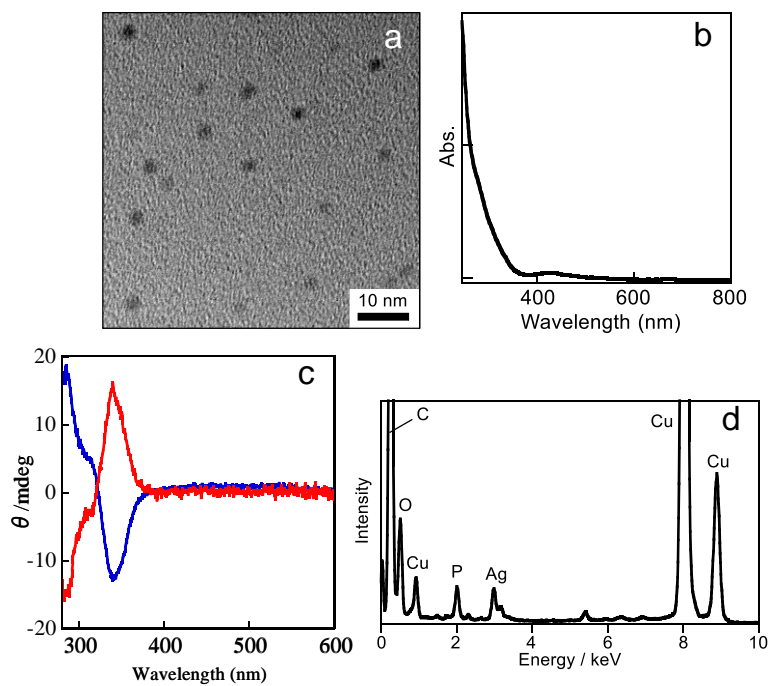


Figure S6. 1-Ag NPs: a) TEM image, b) UV-vis spectrum in CH_2Cl_2 , c) CD spectra in CHCl_3 , and d) EDX spectrum. Cu peaks are from the supporting copper grid.

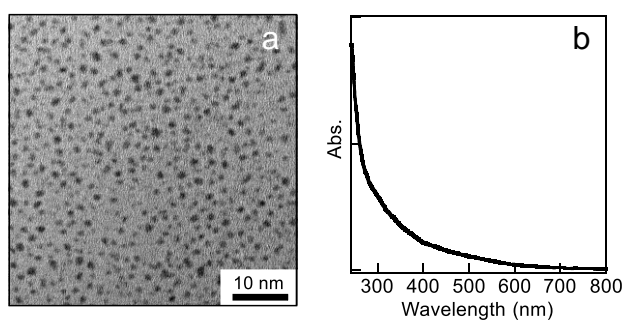


Figure S7. $\text{Ph}_3\text{P-Au}$ NPs: a) TEM image (scale bar = 10 nm) and b) UV-vis spectrum (CH_2Cl_2).

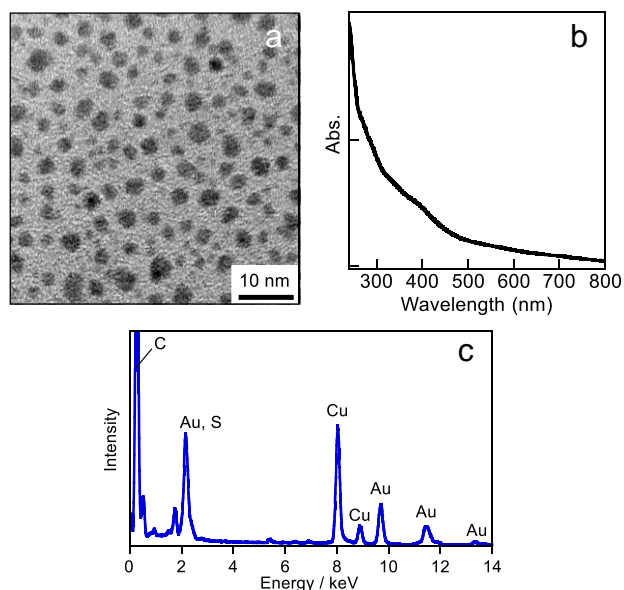


Figure S8. *RS-AuNP* formed from the ligand exchange of $\text{Ph}_3\text{P-Au}$ NPs with octanethiol: a) TEM image (scale bar = 10 nm), b) UV-vis spectrum (CH_2Cl_2), and c) EDX spectrum. Cu peaks are from the supporting copper grid.

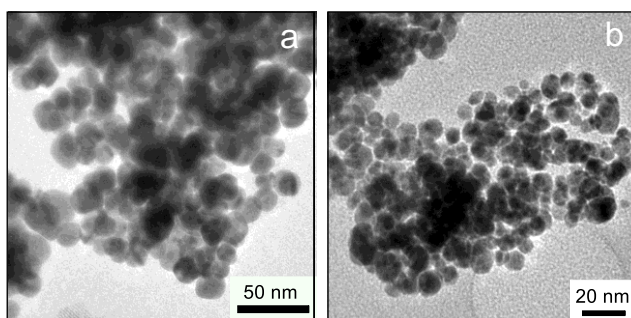


Figure S9. TEM images of a): $\text{Ph}_3\text{P-Au}$ NPs after heating (1 h) [scale bar = 50 nm] and b): BINAP-Au NPs after heating (24 h) [scale bar = 20 nm].

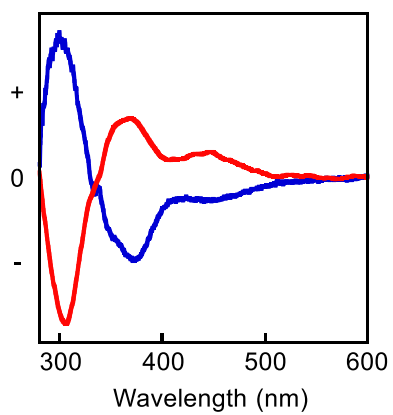


Figure S10. CD spectra (CHCl_3) of (*R*)-1-Au NPs (red line) and (*S*)-1-Au NPs (blue line) after heating (24 h).